A study of the phase transitions and proton dynamics of the superprotonic conductor $Cs_5H_3(SO_4)_4 \cdot 0.5H_2O$ single crystal with ^{1}H and [133]Cs nuclear magnetic resonance

Ae Ran Lim*

Department of Science Education, Jeonju University, Jeonju 560-759, Republic of Korea

Abstract

The phase transitions and proton dynamics of $Cs_5H_3(SO_4)_4 \cdot 0.5H_2O$ single crystals were studied by measuring the NMR line shape, the spin-lattice relaxation time, T_1, and the spin–spin relaxation time, T_2, of the ^{1}H and [133]Cs nuclei. The "acid" protons and the "water" protons in $Cs_5H_3(SO_4)_4 \cdot 0.5H_2O$ were distinguished. The loss of water protons was observed above T_{C1}, whereas the content of water protons was found to recover above T_{C2}. Therefore, the water protons play a special role in the stability of the superprotonic phase at high temperatures. The mechanism of fast proton conduction was found to consist of hydrogen-bond proton transfer involving the breakage of the weak part of the hydrogen bond and the formation of a new hydrogen bond. Thus, these structural phase transitions probably involve significant reorientation of the SO_4 tetrahedra and dynamical disorder of the hydrogen bonds between them.
© 2008 Elsevier Inc. All rights reserved.

1. Introduction

Research into fuel cells for combustion engines and electric power generation is very active because of their high efficiencies and low pollution levels. The search for electrolyte materials suitable for the temperature range between 373 and 573 K is one of the keys to beginning a new generation of fuel cells, because the operating temperature of polymer electrolyte membrane fuel cells is limited to below 373 K by the necessity for a humid atmosphere [1–3]. Proton conduction occurs in several types of materials including many hydrogen-bonded systems. It is well known that high proton conductivity is observed in the high-temperature phases of solid acid salts such as $MHXO_4$, $M_3H(XO_4)_2$, and $M_5H_3(XO_4)_4 \cdot H_2O$ (M = Rb, Cs, NH₄; X = S, Se) [4–9]. Pentacesium trihydrogen tetrasulfate hydrate, $Cs_5H_3(SO_4)_4 \cdot H_2O$, belongs to

the family of protonic superionic conductors with the general formula $M_5X_3(XO_4)_4 \cdot xH_2O$ ($0 \leqslant x \leqslant 1$). The $Cs_5H_3(SO_4)_4 \cdot H_2O$ crystal has a highly symmetric hexagonal structure even at room temperature, unlike the other crystals in this family [10]. This crystal undergoes two phase transitions at 360 and 414 K. The high temperature crystalline phase above 414 K exhibits a much higher conductivity (up to $10^{-1}\Omega^{-1}\,cm^{-1}$) [11]. The phase transition at 414 K is first-order, but the symmetry class and structure of the high conducting phase are not yet precisely known. The phase transition at 360 K from $P6_3/mmc$ to $P6_3/mmc$ is isostructural, and is associated with changes in the local symmetry of the SO_4 tetrahedra [12].

The properties of $Cs_5H_3(SO_4)_4 \cdot H_2O$ crystals have previously been studied by several groups: their structure was analyzed with X-ray diffraction [13,14], the conductivity mechanism was studied with dielectric measurements [11,13] and neutron scattering [15], and the vibration spectrum was investigated with IR, Raman, Brillouin, and neutron scattering over a wide temperature range [16–20].

*Fax: +82 63 220 2053.
E-mail addresses:* aeranlim@hanmail.net, arlim@jj.ac.kr

Further, Fajdiga-Bulat et al. [21] concluded from nuclear magnetic resonance (NMR) results that the appearance of a "liquid-like" proton T_2 above 414 K demonstrates the presence of fast protonic conductivity in $Cs_5H_3(SO_4)_4 \cdot H_2O$. Suzuki and Hayashi [3] recently reported that the superprotonic phase transitions of the hydrated $(Cs_5H_3(SO_4)_4 \cdot 0.5H_2O)$ and anhydrous $(Cs_5H_3(SO_4)_4)$ forms both occur at 420 K. The proton dynamics of $Cs_5H_3(SO_4)_4 \cdot 0.5H_2O$ were studied by determining the ^{1}H static NMR spectra and the spin-lattice relaxation time, T_1. They reported that in both the room temperature and high temperature phases, translational diffusion of protons occurs. The protons in both phases diffuse faster in the hydrated form than in the anhydrous form.

As protons are expected to play a dominant role in the physical properties and phase transition mechanisms of these hydrogen-bonded crystals, probing their proton motions with ^{1}H NMR is expected to be a powerful means of studying their microscopic nature. The relationship between the dynamic transfer of hydrogen atoms and structural phase transitions has been a subject of keen interest. In this connection, the acid and water protons of $Cs_5H_3(SO_4)_4 \cdot 0.5H_2O$ single crystals are particularly worthy of study. The water protons can be distinguished from the acidic protons with the use of solid state NMR methods. In an attempt to elucidate the mechanisms of the structural phase transitions of $Cs_5H_3(SO_4)_4 \cdot 0.5H_2O$, we characterized the dynamics of the acid and water protons in this crystal by measuring the spin-lattice relaxation time, T_1, and the spin–spin relaxation time, T_2. In this paper, the temperature dependences of T_1 and T_2 for the ^{1}H and [133]Cs nuclei in $Cs_5H_3(SO_4)_4 \cdot 0.5H_2O$ single crystals are discussed with particular emphasis on the role within the phase transition mechanisms of the acid and water protons. The results of the present study are significantly different to those of previous studies, especially with regard to the influences of the acid protons, the crystalline water, and the cesium nuclei.

2. Crystal structure

At room temperature, $Cs_5H_3(SO_4)_4 \cdot xH_2O$ crystals are hexagonal with space group $P6_3/mmc$, and the lattice constants are $a = 6.2455$ Å and $c = 29.690$ Å, with $Z = 2$ [22]. The hexagonal structure of $Cs_5H_3(SO_4)_4 \cdot xH_2O$ is shown in Fig. 1. The H_2O molecules are located between the SO_4 layers, and the layers of SO_4 tetrahedra linked by hydrogen bonds are located in the basal plane. This crystal undergoes two successive phase transitions at $T_{C1} = 360$ K and $T_{C2} = 414$ K [23,24]. The phases are denoted I, II, and III in order of descending temperature. The structure of the phase I is unknown, but a possible structure has been suggested by Yuzyuk et al. [16]; the crystal structure of phase I is hexagonal and belongs to $P6/mmm$ with $Z = 1$. The lattice parameter is half the corresponding c_h^{III} and $a_h^I = a_h^{III}$ [10,16]. At T_{C2}, the superionic phase transition is accompanied by the symmetry change $P6/mmm$–$P6_3/mmc$
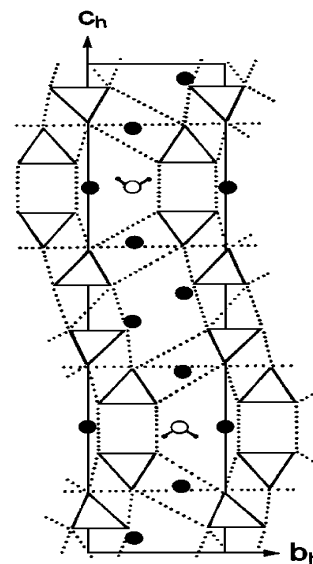

Fig. 1. The hexagonal structure of a $Cs_5H_3(SO_4)_4 \cdot 0.5H_2O$ single crystal on the [100] direction at room temperature (close circles: Cs, dotted lines: H–bonds, tetrahedron: SO_4, and open circles: H_2O).

[17,22], and at T_{C1} an isostructural phase transition occurs, associated with changes in the local symmetry of the SO_4 tetrahedra [10,12,23]. As the temperature decreases, the dynamic disorder of the hydrogen bond network gives way to static disorder (both orientational and positional), and in the vicinity of $T_g = 260$ K a transformation into a proton glass-like phase occurs [25,26].

3. Experimental method

Colorless and transparent single crystals of $Cs_5H_3(SO_4)_4 \cdot 0.5H_2O$ were grown by slow evaporation of an aqueous solution at room temperature. The crystals obtained had a hexagonal plate-like form. The prepared samples were approximately $5 \times 3 \times 2$ mm^3 in size.

The NMR signals of the ^{1}H and [133]Cs nuclei in the $Cs_5H_3(SO_4)_4 \cdot 0.5H_2O$ single crystals were measured using Bruker 200 FT NMR and 400 FT NMR spectrometers at the Korea Basic Science Institute. The static magnetic fields used were 4.7 and 9.4 T, respectively, and the central radio frequency was set at $\omega_0/2\pi = 200.13$ MHz for the ^{1}H measurements, and at $\omega_0/2\pi = 52.48$ and 104.96 MHz for the [133]Cs nuclei measurements. The ^{1}H and [133]Cs T_1 measurements were performed using a π–t–$\pi/2$ inversion recovery pulse sequence and a $\pi/2$–t–$\pi/2$ saturation recovery pulse sequence with spin-echo detection, respectively. Here, the measurement for [133]Cs with the quadrupole nucleus was conducted only for the central line. The π pulse for ^{1}H was 3 μs and the $\pi/2$ pulse for [133]Cs was 5.5 μs. And, the delay time for ^{1}H and [133]Cs was 3 and 10 s, respectively. The ^{1}H and [133]Cs spin–spin relaxation time, T_2, was determined using a $\pi/2$–t–π pulse sequence with the solid echo method [3]. The NMR measurements were performed in the temperature range 180–430 K. The sample temperatures were maintained at a constant value

by controlling the helium gas flow and the heater current, giving an accuracy of $\pm 0.5\,K$.

4. Experimental results and analysis

In order to determine the phase transition temperatures of $Cs_5H_3(SO_4)_4 \cdot 0.5H_2O$, differential scanning calorimetry (DSC) was carried out on the crystals using a Dupont 2010 DSC instrument. The measurements were performed at a heating rate of $10\,K\,min^{-1}$. Endothermic peaks were observed at 340 K ($= T_{C1}$), 418 K ($= T_{C2}$), and 494 K, as shown in Fig. 2. The first and second peaks correspond to the phase transitions, and the third peak corresponds to the melting of the crystal. The melting temperature of 494 K was defined using optical polarizing microscopy. Our finding of a phase transition at 340 K is not consistent with the phase transition temperature of 360 K that has previously been reported.

4.1. ^1H spin-lattice relaxation and spin–spin relaxation times

The NMR spectrum for the ^1H nuclei in $Cs_5H_3(SO_4)_4 \cdot 0.5H_2O$ was measured as a function of temperature. There are two kinds of protons in the $Cs_5H_3(SO_4)_4 \cdot 0.5H_2O$ structure: the "acid" protons and the "water" protons. In our experimental results, the two proton signals due to the acid and water protons are distinct, as shown in Fig. 3; the lines with stronger and weaker intensities are due to the acid and water protons, respectively. The narrower component is due to the acid protons and the broader component to the water protons. The three acid protons and the one water protons should yield two superimposed lines with intensities in a theoretical ratio of 3:1. The observed ratio of the intensities of the acid and water proton spectra is in agreement with the theoretical ratio.
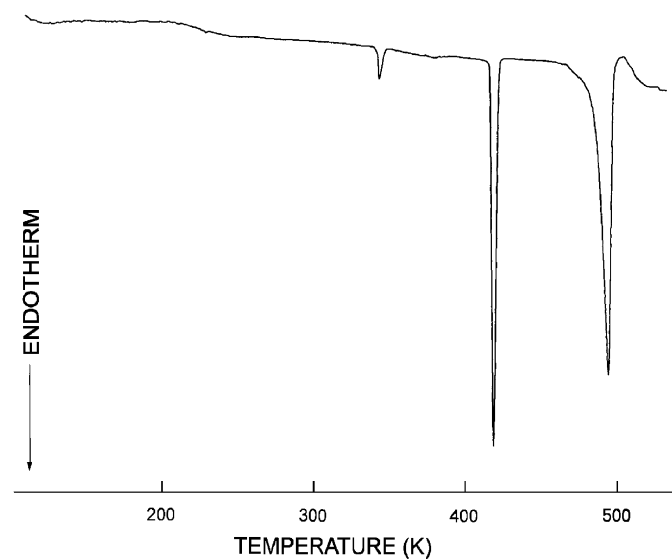

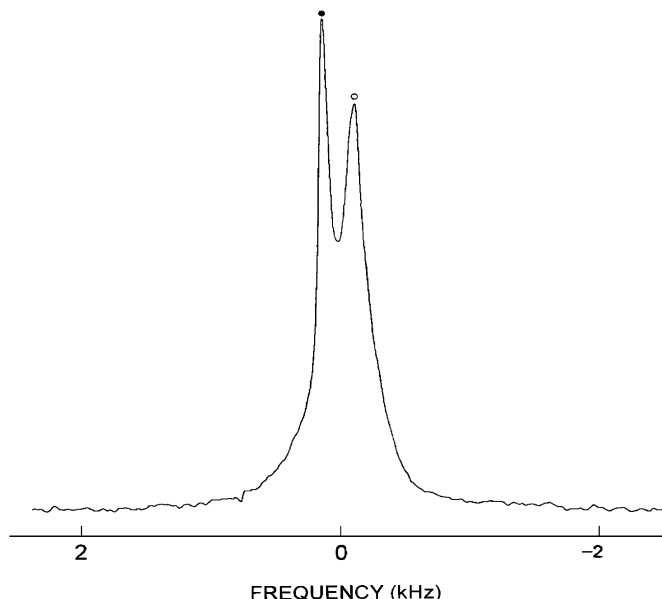Fig. 2. Differential scanning calorimetry (DSC) thermogram of a $Cs_5H_3(SO_4)_4 \cdot 0.5H_2O$ single crystal.

Fig. 3. ^1H NMR spectrum of a $Cs_5H_3(SO_4)_4 \cdot 0.5H_2O$ single crystal at room temperature (●: acid proton and ○: water proton). Here, the numbers of scan and the pulse delay time was 8 and 3 s, respectively, at the Larmor frequency 200.13 MHz.

The line-width due to the acid protons does not vary significantly as a function of temperature, but the signal intensity for the water protons decreases with increasing temperature. This means that the loss of water protons with increasing temperature.

The ^1H spin-lattice relaxation time, T_1, and the spin–spin relaxation time, T_2, were obtained for $Cs_5H_3(SO_4)_4 \cdot 0.5H_2O$ at a frequency of 200.13 MHz. The inversion recovery traces of the magnetizations of ^1H were measured at several different temperatures. The measured magnetization recoveries were found to be satisfactorily fitted with the single exponential function [27,28]

$$\frac{[S(\infty) - S(t)]}{2S(\infty)} = \exp(-Wt), \qquad (1)$$

where $S(t)$ is the nuclear magnetization at time t, and W is the transition probability corresponding to $\Delta m = \pm 1$. The relaxation rates are given by

$$\frac{1}{T_1} = W. \qquad (2)$$

The temperature dependences of T_1 and T_2 for the acid and water protons in $Cs_5H_3(SO_4)_4 \cdot 0.5H_2O$ crystals are shown in Fig. 4. T_1 is more or less continuous at T_{C1} ($= 340\,K$), which suggests that the crystal lattice does not change very much in this transition, and that it is not affected by the acid or water protons. The abrupt changes in the temperature dependence of T_1 near 418 K are associated with the phase transition. Thus, the crystal lattice probably changes significantly during the phase transition at 418 K. The proton spin–spin relaxation time, T_2, was measured using the solid echo method, and the data for the temperature interval between 200 and 430 K
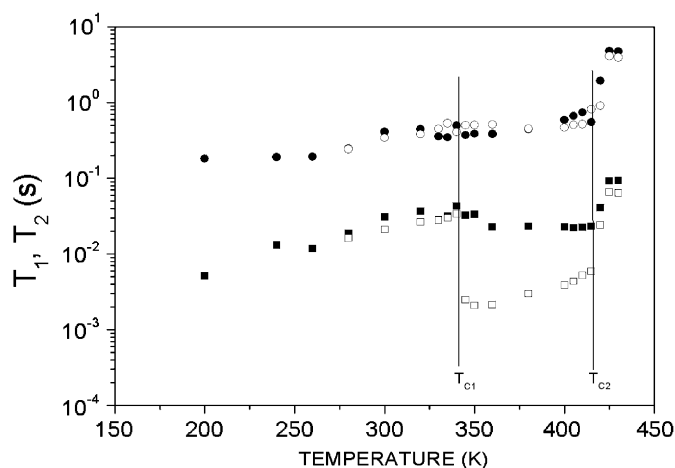
Fig. 4. Temperature dependences of T_1 and T_2 for acid and water protons in a $Cs_5H_3(SO_4)_4 \cdot 0.5H_2O$ single crystal ($\bullet$: T_1 and $\blacksquare$: T_2 for acid proton, $\circ$: T_1 and $\square$: T_2 for water proton).

Fig. 5. ^{133}Cs NMR spectrum of a $Cs_5H_3(SO_4)_4 \cdot 0.5H_2O$ single crystal at room temperature. Here, the numbers of scan and the pulse delay time was 64 and 10 s, respectively, at the Larmor frequency 104.96 MHz.

are displayed in Fig. 4. Near T_{C1}, T_2 for the water protons abruptly decreases, whereas T_2 for the acid protons remains nearly constant. The reason for the abrupt decrease in T_2 for the water protons near T_{C1} is possibly the loss of crystalline water at this temperature. The motions of the acid and water protons in the phase I are thus liquid-like, so the dipolar interaction between the protons is averaged out to zero. Thus, T_2 abruptly increases in phase I, the fast-ion conductor phase. This situation is analogous to that for $CsHSO_4$ [29]. This result demonstrates the presence of translational diffusion in addition to molecular rotation in the superprotonic phase, which results in the high mobility of protons above T_{C2}.

4.2. ^{133}Cs spin-lattice relaxation and spin–spin relaxation times

The NMR spectrum of ^{133}Cs ($I = 7/2$) at room temperature is shown in Fig. 5. Seven resonance lines, comprised of a strong central line and six well-resolved satellite lines, were observed when the magnetic field was applied along an arbitrary direction. In this figure, the zero point of the x-axis is the resonance frequency, 104.96 MHz, of the ^{133}Cs nucleus. Over the temperature range 300–430 K, the central transition is almost unshifted by the quadrupole interaction, and the resonance line splitting between the satellite lines varies with temperature. The splitting of the ^{133}Cs resonance line changes discontinuously at the phase transition temperatures 340 and 418 K, as shown in Fig. 6; these sudden changes in the splitting of the Cs resonance line can be attributed to changes in the local symmetry at the ^{133}Cs site during the phase transitions. The changes in the line positions indicate that the electric field gradient (EFG) at the ^{133}Cs sites varies with temperature, which in turn indicates that the atoms neighboring the ^{133}Cs atoms are displaced during the phase transitions. The results for the Cs resonance lines show that the ^{133}Cs quadrupole coupling constants in phases I, II,
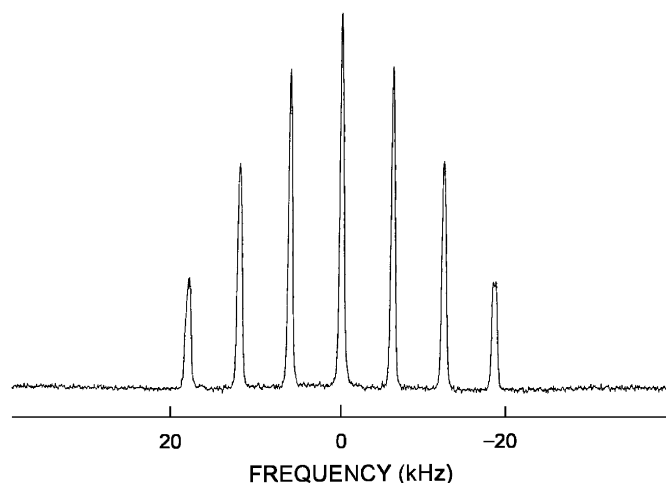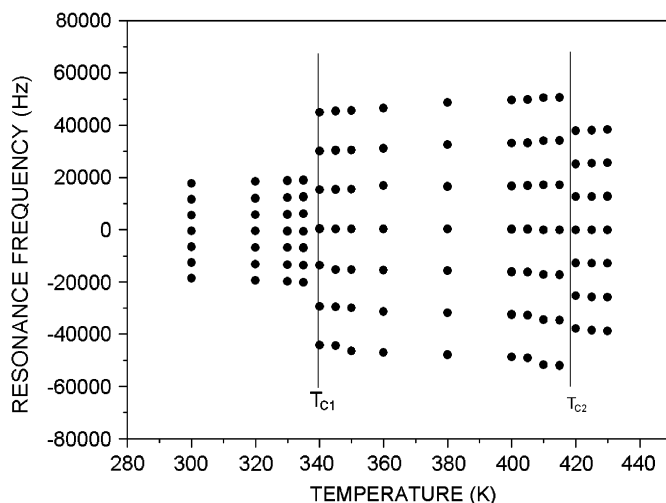

Fig. 6. The splitting of the ^{133}Cs resonance lines as a function of temperature.

and III are different from each other; the quadrupole coupling constant in phase III is smaller than the quadrupole coupling constant in phase II, and the quadrupole coupling constant in phase II is larger than the quadrupole coupling constant in phase I. Thus, the Cs ions play an important role in the I–II and II–III phase transitions. Usually, the quadrupole coupling constant decreases as a function of increasing temperature in many materials [30,31]. However, the quadrupole coupling constant of ^{133}Cs in $Cs_5H_3(SO_4)_4 \cdot 0.5H_2O$ increases in phase II, in contrast to the general decreasing trend. The origin of this increasing trend of the quadrupole coupling constant with increasing temperature is not understood.

The spin-lattice relaxation times of ^{133}Cs in $Cs_5H_3(SO_4)_4 \cdot 0.5H_2O$ were measured at the frequency of 52.48 MHz. The recovery traces of the magnetization were determined for this crystal at several different temperatures. In the case of dominant quadrupole relaxation such

as for $Cs_5H_3(SO_4)_4 \cdot 0.5H_2O$, the recovery trace of the central line of ^{133}Cs is not single exponential, but can be represented by a combination of four exponential functions. The signal for $W_1 = W_2$ is given by [32–34]

$$\frac{[S(\infty) - S(t)]}{S(\infty)}$$

$$= 0.048 \exp(-0.476 W_1 t) + 0.818 \exp(-1.333 W_1 t)$$
$$+ 0.050 \exp(-2.381 W_1 t) + 0.084 \exp(-3.810 W_1 t), \quad (3)$$

where $S(t)$ is the nuclear magnetization corresponding to the central transition at time t, and W_1 and W_2 are the transition probabilities corresponding to $\Delta m = \pm 1$ and $\Delta m = \pm 2$, respectively. The return to equilibrium is characterized by four relaxation times.

We determined the variations with temperature of the relaxation times for the central resonance line of the ^{133}Cs nuclei. The spin-lattice relaxation time was obtained with the saturation method. The ^{133}Cs relaxation time was obtained in terms of W_1 using Eq. (3), and the temperature dependences of the ^{133}Cs spin-lattice relaxation time, T_1, and the spin–spin relaxation time, T_2, are shown in Fig. 7. Here, T_1 and T_2 did not change during the heating and cooling in NMR. From the temperature dependence on T_1 and T_2, we know that transformation between two phase transitions of $Cs_5H_3(SO_4)_4 \cdot 0.5H_2O$ single crystals is quasi-reversible. The spin-lattice relaxation times for ^{133}Cs are very long in phases III and II. T_1 of the ^{133}Cs nuclei was found to undergo significant changes near T_{C1} and T_{C2}, and these changes coincide with the changes in the splitting of the ^{133}Cs resonance lines. Further, these changes in the temperature dependences of T_1 and T_2 at T_{C1} and T_{C2} for the ^{133}Cs nuclei coincide with the changes in the behaviors of T_1 and T_2 for the ^1H nuclei at the same temperature. Abrupt changes in relaxation times are associated with structural phase transitions. Here, T_2 is nearly constant as a function of temperature, and is of the order of several milliseconds, i.e., liquid-like.

Fig. 7. Temperature dependences of T_1 and T_2 for ^{133}Cs in a $Cs_5H_3(SO_4)_4 \cdot 0.5H_2O$ single crystal.

5. Discussion and conclusion

The phase transitions and proton dynamics of $Cs_5H_3(SO_4)_4 \cdot 0.5H_2O$ were studied by means of ^1H and ^{133}Cs solid state NMR. The phase transition temperatures 340 and 418 K were established with DSC, and these results are consistent with the results 340 and 418 K obtained with NMR. The changes in the ^1H and ^{133}Cs spin-lattice and spin–spin relaxation times at T_{C1} (= 340 K) and T_{C2} (= 418 K) are due to the fact that the environments of the ^1H and ^{133}Cs nuclei change only during these transitions.

Two kinds of protons in the $Cs_5H_3(SO_4)_4 \cdot 0.5H_2O$ structure were identified: the "acid" protons and the "water" protons. Our experimental results show that the acid and water protons are involved in the phase transitions. A loss of water protons was observed above T_{C1}; the dehydration of the crystal at T_{C1} take place in investigated crystal. However, the rate of process is limited by the diffusion of water in the bulk and through the surface of single crystal sample. Therefore, the water protons play a special role at high temperatures in the stabilities of the superprotonic phase, which has a $Cs_5H_3(SO_4)_4 \cdot 0.5H_2O$ dynamically disordered hydrogen bond network. This result is similar to that for $K_9H_7(SO_4)_8 \cdot H_2O$ reported by Vrtnik et al. [35]. The phase transition near 418 K leads to a superionic phase, as shown by its "liquid-like" characteristics. The liquid-like value of the proton T_2 is compatible with the suggestion that the phase above T_{C2} is superionic [13,25]. The ^1H T_1 and T_2 results show that in its high-temperature phase the $Cs_5H_3(SO_4)_4 \cdot 0.5H_2O$ crystal is a fast-ionic conductor; this behavior is expected for most hopping-type ionic conductors, and is attributed to interactions between the mobile ions and the neighboring group ions within the crystal. The mechanism of this fast proton conduction at high temperatures probably involves the breaking of hydrogen bonds between the nearest SO_4 tetrahedra and the forming of new weaker disordered hydrogen bonds between neighboring SO_4 tetrahedra. Further, this structural phase transition may involve significant reorientation of the SO_4 tetrahedra and the dynamical disorder of the hydrogen bonds between them. Fast rotation of the SO_4 tetrahedra also results in breaking of the water bonding, so the water molecules are freed and diffuse out of the crystal [3,34]. The fluctuations of the EFG at the Cs sites in $Cs_5H_3(SO_4)_4 \cdot 0.5H_2O$ single crystals that are responsible for the observed T_1 and quadrupole coupling constant anomalies originate mainly from variations in the motions of the nearest neighboring oxygen atoms. We suggest that shifts in the positions of the oxygen atoms in the sulfate groups around the Cs atoms also play an important role in these phase transitions. The previously report was for the "acid" protons in $Cs_5H_3(SO_4)_4$ and the "water" protons in $Cs_5H_3(SO_4)_4 \cdot 0.5H_2O$, respectively. In present work, the "acid" protons and the "water" protons in $Cs_5H_3(SO_4)_4 \cdot 0.5H_2O$ single crystals were distinguished. Our NMR study has provided new information about the roles of acid
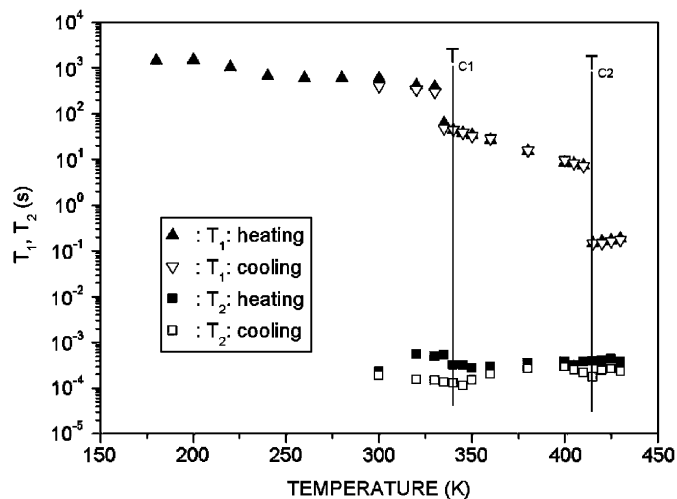
protons, water protons, and cesium nuclei in $Cs_5H_3(SO_4)_4 \cdot 0.5H_2O$ single crystals.

Acknowledgment

References

[1] M. Haile, D.A. Boysen, C.R.I. Chisholm, R.B. Merle, Nature 410 (2001) 910.
[2] A.R. Lim, J.H. Chang, H.J. Kim, H.M. Park, Solid State Commun. 129 (2004) 123.
[3] K.I. Suzuki, S. Hayashi, Phys. Rev. B 74 (2006) 134303.
[4] A.I. Baranov, L.A. Shuvalov, N.M. Schagina, JETP Lett. 36 (1982) 381.
[5] A. Pawlowski, C.Z. Pawlaczyk, Ferroelectrics 81 (1988) 201.
[6] A.I. Baranov, E.D. Yakushkin, D.J. Jones, J. Roziere, Solid State Ionics 125 (1999) 99.
[7] Y. Matsumoto, J. Phys. Soc. Japan 70 (2001) 1437.
[8] A.I. Baranov, Ferroelectrics 265 (2002) 87.
[9] A.R. Lim, Phys. Rev. B 72 (2005) 64103.
[10] Y.I. Yuzyuk, V.P. Dmitriev, V.V. Loshkarev, L.M. Rabkin, L.A. Shuvalov, Cryst. Rep. 39 (1994) 61.
[11] O.A. Kabanov, Dissertation Institute of Crystallography, Russian Academy of Science, Moscow, 1993.
[12] S.G. Lushnikov, V.H. Schmidt, L.A. Shuvalov, V.V. Dolbinina, Solid State Commun. 113 (2000) 639.
[13] A.I. Baranov, O.A. Kabanov, B.V. Merinov, L.A. Shuvalov, Ferroelectrics 127 (1992) 257.
[14] B.V. Merinov, A.I. Baranov, L.A. Shuvalov, J. Schneider, H. Schulz, Solid State Ionics 69 (1994) 153.
[15] A.V. Belushkin, C.J. Carlile, L.A. Shuvalov, Ferroelectrics 167 (1995) 21.
[16] Y.I. Yuzyuk, V.P. Dimitriev, V.V. Loshkarev, L.M. Rabkin, L.A. Shuvalov, Ferroelectrics 167 (1995) 53.
[17] Y.I. Yuzyuk, V.P. Dmitriev, L.M. Rabkin, P. Smutny, J. Phys.: Condens. Matter 8 (1996) 3965.
[18] F. Kadlec, Y. Yuzyuk, P. Simon, M. Pavel, Ferroelectrics 176 (1996) 179.
[19] A.V. Belushkin, M. Bull, C. Carlile, S.G. Lushnikov, Physica B 241–243 (1998) 484.
[20] A.I. Fedoseev, S.G. Lushnikov, J.H. Ko, S. Kojima, L.A. Shuvalov, Solid State Phenomena 115 (2006) 279.
[21] A.M. Fajdiga-Bulat, G. Lahajnar, J. Dolinsekk, J. Slak, B. Lozar, B. Zalar, L.A. Shuvalov, R. Blinc, Solid State Ionics 77 (1995) 101.
[22] B.V. Merinov, A.I. Baranov, L.A. Shuvalov, J. Schneider, H. Schulz, Solid State Ionics 74 (1994) 53.
[23] S.G. Lushnikov, L.A. Shuvalov, Crystallogr. Rep. 44 (1999) 615.
[24] A.M. Fajdiga-Bulat, F. Romain, M.H. Limage, A. Lautie, J. Mol. Str. 326 (1994) 93.
[25] A.I. Baranov, O.A. Kabanov, L.A. Shuvalov, JEPT Lett. 58 (1993) 548.
[26] Y. Yuzyuk, V. Dmitriev, L. Rabkin, L. Burmistrova, L. Shuvalov, F. Smutny, P. Vanek, I. Gregora, J. Petzelt, Solid State Ionics 77 (1995) 122.
[27] A. Abragam, The Principles of Nuclear Magnetism, Oxford University Press, Oxford, 1961.
[28] A.R. Lim, J.K. Jung, S.Y. Jung, J. Phys. Chem. Solids 63 (2002) 625.
[29] A. Damyanovich, M.M. Pintar, R. Blinc, J. Slak, Phys. Rev. B 56 (1997) 7942.
[30] A.A. Koukoulas, M.A. Whitehead, Chem. Phys. Lett. 167 (1990) 379.
[31] R.J.C. Brown, J. Chem. Phys. 53 (1990) 3247.
[32] E.R. Andrew, D.P. Tunstall, Proc. Phys. Soc. (London) 78 (1961) 1.
[33] D.P. Tewari, G.S. Verma, Phys. Rev. 129 (1963) 1975.
[34] M.A. Gordon, M.J.R. Hoch, J. Phys. C: Solid State Phys. 11 (1978) 783.
[35] S. Vrtnik, T. Apih, M. Klanjsek, P. Jeglic, G. Lahajnar, L.F. Kirpichnikova, A.I. Baranov, J. Dolinsek, J. Phys.: Condens. Matter 16 (2004) 7967.